Applied Geochemistry 84 (2017) 348–359

Contents lists available at ScienceDirect

Applied Geochemistry

journal homepage: www.elsevier.com/locate/apgeochem

Does sorption influence isotope ratios of chlorinated hydrocarbons under field conditions?

Philipp Wanner [a, b, *], Beth L. Parker [b], Steven W. Chapman [b], Ramon Aravena [c], Daniel Hunkeler [a]

[a] Centre for Hydrogeology & Geothermics (CHYN), University of Neuchâtel, Rue Emil Argand 11, CH-2000 Neuchâtel, Switzerland
[b] G360 Institute for Groundwater Research, College of Engineering and Physical Sciences, University of Guelph, 50 Stone Road East, Guelph, Ontario N1G 2W1, Canada
[c] Department of Earth and Environmental Sciences, University of Waterloo, 200 University Avenue West, Waterloo, Ontario N2L 3GI, Canada

ARTICLE INFO

Article history:
Received 5 February 2017
Received in revised form
4 July 2017
Accepted 25 July 2017
Available online 31 July 2017

Editorial handling by Prof. Khalil Hanna.

ABSTRACT

This study aims to investigate the effect of sorption on isotope ratios of chlorinated hydrocarbons migrating through the subsurface. For this purpose concentration and isotope ratio profiles (carbon and chlorine) were determined in saturated low permeability sediments below two DNAPL sources (1,2-Dichloroethane (1,2-DCA) and Dichloromethane (DCM)). The sources had been emplaced artificially as part of a long-term, emplaced source field experiment 15.5 years (5673 days) ago. Low permeable sediments are well-suited for investigating sorption-induced isotope fractionation under field conditions. The advancing concentration front, where isotope fractionation due to sorption is expected, can be localized precisely and sampled at a high spatial resolution. Along a concentration profile below the 1,2-DCA and DCM DNAPL sources, opposite isotope trends were observed with an enrichment of heavy carbon isotopes ($\Delta\delta^{13}C = 1.9‰$ for 1,2-DCA and 2.4‰ for DCM) and a depletion of heavy chlorine isotopes ($\Delta\delta^{37}Cl = 1.3‰$ for 1,2-DCA). For field data interpretation laboratory experiments were conducted to determine sorption and diffusion-induced isotope fractionation factors for 1,2-DCA and DCM and included in a numerical model. When considering only diffusive isotope fractionation, numerical simulation failed to reproduce the opposite isotope trends. In contrast when sorption-induced isotope fractionation was also included, the model reproduced the data well. Hence, the observed isotope trends reflect a superposition between competing isotope effects due to sorption and diffusion. For chlorine the diffusive isotope effect is larger than for carbon due to the mass difference of two between the stable isotopes overruling the sorption effect, while for carbon the sorption effect dominates. The observed shifts of isotope ratios due to sorption are in the range of the 2‰ threshold value, which is often used for identifying reactive processes. Numerical modelling showed that under specific conditions (strong sorption behavior, early transient diffusion) even higher shifts of isotope ratios can occur. Hence, when shifts of isotope ratios in the range of 2‰ are observed under field conditions where sorption prevails, their attribution to reactive processes should be made with caution. This is especially crucial if a reactive process is slow and associated with a small isotope fractionation factor.

1. Introduction

Chlorinated hydrocarbons are common subsurface contaminants at many polluted sites throughout the world (Aelion et al., 2010; Pankow and Cherry, 1996). As a result of improper disposal and accidental spills, chlorinated hydrocarbons are often released at the surface as dense non-aqueous phase liquid (DNAPL) and migrate downwards into aquifer systems due to their high mobility (high density, low viscosity) (Pankow and Cherry, 1996; Schwille, 1988). Chlorinated hydrocarbons tend to accumulate on top of low permeability layers (e.g. aquitards) and are slowly dissolved creating a persistent contaminant plume (Hwang et al., 2008; Kueper et al., 1993). With increasing time, the accumulated

* Corresponding author. G360 Institute for Groundwater Research, College of Engineering and Physical Sciences, University of Guelph, 50 Stone Road East, Guelph, ON N1G 2W1, Canada.
E-mail address: philipp.wanner@g360group.org (P. Wanner).

http://dx.doi.org/10.1016/j.apgeochem.2017.07.016
0883-2927/

chlorinated hydrocarbons are transported by diffusion into the underlying low permeability layer (Chapman and Parker, 2005; Parker, 1996; Parker et al., 2008). During the migration in aquifers and low permeable units, chlorinated hydrocarbons are retarded due to sorption, which affects the migration rate and spreading of the contaminants (Allen-King et al., 1996; Parker et al., 1994; Rivett and Allen-King, 2003).

Stable isotope methods have been widely applied to gain insight into the origin and fate of organic compounds in the subsurface (Elsner et al., 2005; Harrington et al., 1999; Huang et al., 1999; Hunkeler et al., 2011, 2005, 1999; Jeannottat and Hunkeler, 2012; Jeannottat and Hunkeler, 2013; Lollar et al., 1999; Meckenstock et al., 2004; Wanner and Hunkeler, 2015; Wanner et al., 2016). Researchers have shown that aqueous phase diffusion can cause isotopic fractionation in aquifer – aquitard systems (Wanner and Hunkeler, 2015). However, there is currently no consensus on whether sorption results in significant isotope fractionation under field conditions, partly due to the lack of field data at sufficiently high spatial resolution. In analytical chemistry, it is known that liquid chromatographic separation of organic compounds is associated with an isotope effect. Light isotopes are preferentially sorbed on the stationary phase leading to an enrichment of heavy isotopes in the mobile phase (Caimi and Brenna, 1993, 1997; Filer, 1999; Klein et al., 1964; Poulson et al., 1997). In contrast, less is known about isotope effects of chlorinated hydrocarbons during sorption in natural systems. Some laboratory studies suggested that sorption might not alter isotope ratios (Schüth et al., 2003; Slater et al., 2000), while others provided evidence for significant sorption-induced isotope fractionation (Höhener and Yu, 2012; Imfeld et al., 2014; Kopinke et al., 2005). To extrapolate from the laboratory to the field scale, modeling studies have been used so far (Höhener and Atteia, 2010; Liu et al., 2016; Van Breukelen and Prommer, 2008). The simulations revealed a significant isotope effect due sorption, especially at the fringe of contaminant plumes, which potentially complicates the assessment of reactive processes using stable isotope methods (Van Breukelen and Prommer, 2008). However, it is challenging to gather field evidence for sorption-induced isotope fractionation, as it is difficult to localize and to sample the plume fringe, where isotope fractionation is predicted, at sufficient high spatial resolution. Furthermore, at the plume fringe, isotope fractionation might also occur due to mixing enhanced degradation and diffusion across the steep concentration gradient, which complicates an unequivocal interpretation of isotope patterns. In contrast to aquifers, low permeable units offer several advantages for investigating sorption-induced isotope fractionation: a) the diffusion front can be targeted very precisely and sampled at a very high spatial resolution, b) the retardation due to sorption is expected to be stronger due to the higher organic carbon content typical of fine-grained clay-rich sediments (i.e. clayey aquitards) compared to granular aquifers, and c) the transport mechanisms are well constrained, while in case of dispersion in sandy aquifers, the diffusion contribution often remains unclear, which introduces greater uncertainty in the data evaluation.

The aim of this study is to investigate whether sorption has a significant influence on isotope ratios of chlorinated hydrocarbons under field conditions. The study was done as a part of a long-term controlled field experiment in well-characterized saturated low permeability sediments (Johnson et al., 1989; Parker, 1996) showing a strong sorption behavior (Allen-King et al., 1995, 1996, 1997). The controlled-release experiment was initiated by emplacing between 1.5 and 2 L of different chlorinated solvents (Tetrachchloroethene (PCE), Trichloroethene (TCE), Dichloromethane (DCM), 1,2-Dichloroethane (1,2-DCA) and TCE/DCM mixture) as DNAPL in boreholes drilled into the low permeable unit to depths of between 10 and 12 m below ground surface (bgs), were no visible fractures were present (Parker, 1996). For the present study, cores were retrieved 15.5 years (5673 days) after DNAPL emplacement beneath the 1,2-DCA and the DCM DNAPL sources to determine concentration and isotope ratio profiles (C and Cl) for evaluating sorption-induced isotope fractionation at the field scale. For field data interpretation, isotope fractionation factors for sorption and diffusion were determined in the laboratory and included in a numerical model to simulate observed isotope ratio profiles. Finally, it was investigated to what extent sorption-induced isotope fractionation impairs the identification of reactive processes by using stable isotope methods.

2. Materials and methods

2.1. Multistep sorption experiment

In the laboratory, isotope fractionation due to sorption was quantified by using a multistep approach, which leads to a higher shift of isotope ratios and thus, to a higher precision of the determined isotope fractionation factor compared to a single step batch experiment. Two replicates of multistep sorption experiments were performed for 1,2-DCA and DCM with initial concentrations of 7226 mg/L and 5983 mg/L for 1,2-DCA and of 572 mg/L and 745 mg/L for DCM, respectively. The experiment included five sorption steps until the concentration in the solution was too low to determine the concentration and isotope ratios. In a 42 mL vial, 30 mL of solution with 1,2-DCA or DCM were mixed with 15 g of dry uncontaminated clay from the field site (see site description in section 2.3.). To ensure the representativeness of the clay samples, they were taken from the same coring location as the clay cores at the site but at a greater depth, where no contaminants were detected. Before adding the clay samples to the 42 mL vials, they were dried for a week at 40 °C and subsequently pulverized by hand with a mortar. The vials containing the clay samples and solution were shaken on a rotary shaker for 24 h. This equilibration time was chosen based on previous studies, which also applied a multistep approach to quantify sorption-induced isotope fractionation (Imfeld et al., 2014, Kopinke et al., 2005) or characterized sorption using clay material from the same site (Johnson et al., 1989) or from other sites with similar material (Grathwohl, 1990). After each sorption step, an aliquot (4 mL) of the solution was removed from the vials for concentration and isotope ratio analyses and 10 mL of the solution was removed from the vial with a pipette and added to the subsequent 42 mL vial containing a new 15 g dried clay sample and 20 mL of deionized water for the next sorption step. The transfer was conducted by completely submersing the pipette into the 20 mL of water in the subsequent vial to avoid volatilization during the transfer. Due to the small headspace volume (4.5 mL), the mass loss due to volatilization was lower for 1,2-DCA (0.5%) and for DCM (1.1%) than the uncertainty of the measurement (4% for 1,2-DCA and 5% for DCM, see section 1.4. in Supporting Information). Hence, mass loss due to volatilization and its associated isotope effect can be neglected for determining the sorption-induced isotope fractionation factor. The isotope fractionation factor due to sorption was determined using the equation for multistep experiments derived by Kopinke et al. (2005), Voskamp (2004) and Imfeld et al. (2014):

$$\alpha_{sorption} = \frac{^{H}K_d}{^{L}K_d} \approx 1 + \Delta\delta_i/[1000m(1 - X_{dissolved})] \quad (1)$$

where $^{H}K_d$ and $^{L}K_d$ are the carbon-pore water partitioning coefficients for the heavy and light isotope, respectively, $\alpha_{sorption}$ refers to the fractionation factor due to sorption, $\Delta\delta_i = \delta_{i,final} - \delta_{i,initial}$

refers to the total shift of isotope ratios during the multistep experiment, m corresponds to the number of identical sorption steps and ($1-X_{dissolved}$) is the average amount adsorbed after each sorption step.

The uncertainty of the sorption-induced fractionation factor ($\pm 1\sigma$, eq. (1)) was determined with the Gaussian error propagation law by including the uncertainty of the isotope ratio and the $X_{dissolved}$ measurements.

2.2. Diffusion cell experiment

In addition to sorption, the isotope effect due to aqueous phase diffusion was also quantified, which is required for the interpretation of the field profile isotope data given the simultaneous occurrence of diffusion and sorption in saturated low permeability sediments. The magnitude of isotope fractionation due to aqueous phase diffusion was quantified by using a modified Stokes' diffusion cell as described by Wanner and Hunkeler (2015). For the present study, the diffusion cell experiment was performed for DCM, while for 1,2-DCA the previously reported value was used (Wanner and Hunkeler, 2015). The modified Stokes' diffusion cell corresponds to a Rayleigh type experiment, whereby isotopically heavy and light species are transported by diffusion out of a source reservoir through a small pore sized frit at different diffusive transport rates. The magnitude of isotope fractionation due to different rates of aqueous phase diffusion was quantified by determining the diffusion coefficient ratios between isotopically distinct species using the Rayleigh equation:

$$[ln(R_t/R_0)] \times 1000 = \left(\frac{D_{0,H}}{D_{0,L}} - 1\right) \times 1000 ln\, f \qquad (2)$$

where R_t is the isotope ratio at time t in the source reservoir, R_0 refers to the initial isotope ratio in the source reservoir, $D_{0,H}/D_{0,L}$ is the ratio between diffusion coefficient of the heavy and the light isotope, respectively in free solution and f corresponds to the remaining fraction in the source reservoir.

2.3. Site description and emplaced source field experimental procedure

A detailed description of the long-term emplaced source field experiment is provided in section 1.1. of the Supporting Information. In brief, the emplaced source field experiment was carried out at a permitted hazardous waste disposal site, 15 km southeast from Sarnia, 300 km west of the city of Toronto in Ontario, Canada in the Lambton Clay Plain. At the site, an experimental area was established outside of the active disposal area, with the goal of conducting long-term emplaced source field experiments in the water-saturated low permeability sediments of the Lambton Clay Plain. The well-characterized, regionally extensive water-saturated clay unit of the Lambton Clay Plain underlying this area (Allen-King et al., 1996; Desaulniers et al., 1985; Johnson et al., 1989; McKay and Fredericia, 1995; Myrand et al., 1992; Parker, 1996) can be divided into a weathered upper clay unit with a thickness of about 2.5–3.5 m, transitioning to unoxidized clay with oxidation staining along fractures to a depth of 6–7 m below ground surface (bgs), underlain by a non-weathered, unfractured lower unit with a thickness of about 30 m in which the field experiment was carried out (Fig. 1). The high organic matter content of the aquitard unit (0.534% ± 0.241%; n = 36) strongly retards the migration of organic contaminants due to sorption, with no evidence for degradation over the time-scales of a previous study (Parker, 1996). To perform the long-term controlled release field experiments, different DNAPL sources (PCE, TCE, DCM, 1,2-DCA and TCE/DCM mixture) with volumes between 1.5 and 2.0 L were emplaced approximately 5 m apart in November 1998 in the non-weathered clay at depths of 10–12 m bgs (Fig. 1) in holes created with large diameter Shelby tubes (11.4 cm) for minimal disturbance.

2.4. Core retrieval, subsampling and VOC extractions

A detailed description of core retrieval, core subsampling and VOC extraction from core subsamples is provided in sections 1.2. and 1.3. of the Supporting Information. Briefly, continuous cores were collected from the unweathered clay below the 1,2-DCA and DCM DNAPL sources in June 2014, 15.5 years (5673 days) after source emplacement. The cores were retrieved using a direct push rig using the Envirocore dual tube continuous coring system described by Einarson et al. (1998). After bringing the cores to the surface, the percent recovery was recorded and core tubes were split in half longitudinally and subsampled in the field as a function of depth with narrow spaced sampling points (~5 cm) to gain highly resolved depth-discrete chlorinated hydrocarbon concentration and compound-specific isotope ratio profiles. Subsequently, chlorinated hydrocarbons were extracted into the methanol following the description by Parker (1996) and White et al. (2008) and the total concentrations in the clay were determined based on equation (1) in the Supporting Information.

2.5. Concentration and compound-specific isotope analysis (CSIA)

Detailed descriptions of analytical methods are available in section 1.4. of the Supporting Information. In brief, chlorinated hydrocarbon concentrations in laboratory samples (multistep sorption and diffusion experiment) and in the methanol extracts of the field samples were analyzed by a gas chromatograph coupled to a mass spectrometer (GC-MS). Compound-specific carbon isotope ratios of 1,2-DCA and DCM were analyzed relative to a CO_2 standard by a gas chromatograph coupled to an isotope mass spectrometer (GC-IRMS) and expressed in the delta notation VPDB $\delta = (R/R_{std}-1)*1000$ (‰), where R and R_{std} are the isotope ratios of the sample and the standard, respectively. The analytical uncertainty for samples from the laboratory multistep sorption and diffusion experiment (standard deviation of the mean: SDM = $1\sigma/(n)^{1/2}$ σ: standard deviation n: sample number) was determined based on a triplicate measurement. In contrast, field samples were analyzed only twice due to the limited sample volume. Thus, the standard deviation of the mean (±SDM) for the field samples was estimated based on the standard deviation (1σ) of standards included in the samples sequence ($\sigma = 0.32‰$, n = 12). Compound-specific chlorine isotope ratios were analyzed using a gas chromatograph coupled to a quadrupole mass spectrometer (GC-qMS). Compound-specific chlorine isotope ratios were exclusively determined for 1,2-DCA, since no standards referenced to the SMOC scale (standard mean ocean water) are available for DCM. The 1,2-DCA chlorine isotopic raw ratios were determined from the two most abundant fragment ion peaks (m/z 64 and 62) (Palau et al., 2014; Wanner and Hunkeler, 2015) using an equation that relates fragment ratios to isotope ratios for symmetric molecules developed by (Elsner and Hunkeler, 2008):

$$\left(\frac{^{37}Cl}{^{35}Cl}\right)_{1,2-DCA} = \frac{I_{64}}{I_{62}} \qquad (3)$$

where I is the corresponding fragment ion abundance of 1,2-DCA at different m/z values.

The raw chlorine isotope ratios from 1,2-DCA fragments (eq. (3)) were calibrated against two external standards having different

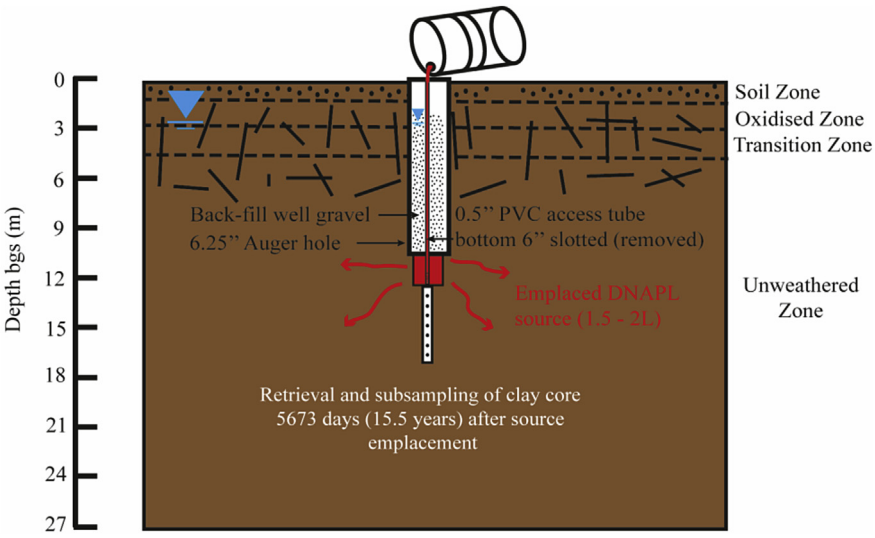

Fig. 1. A cross section of the experimental setup for multiple-year solute diffusion from a constant source concentration (with DNAPL present to ensure aqueous solubility in the adjacent pore water) in the Lambton Clay Plain at the permitted hazardous waste disposal site located close to Sarnia in Ontario, Canada.

chlorine isotope ratios (CHYN1 = 6.30‰ and CHYN2 = −0.84‰) to obtain delta values on the SMOC scale. The standards were characterized by the Holt method (Holt et al., 1997) at the Helmholtz Centre in Munich. The analytical uncertainty (±SDM) of each 1,2-DCA measurement was based on a tenfold measurement of each sample from two different vials (five replicates from each vial).

3. Numerical modelling

The migration of chlorinated hydrocarbons in the clayey unit was simulated in 3 dimensions by rotating a 2D numerical modeling domain around a vertical axis (Fig. 1, Supporting Information). The aim of the simulation was to assess a) how isotope fractionation due to sorption and diffusion are reflected in isotope ratio profiles in water-saturated low permeability sediments, and b) whether observed shifts of carbon and chlorine isotope ratios are reproducible with laboratory determined isotope fractionation factors for diffusion and sorption. A detailed description of the 2D axisymmetrical model is available in section 2. of the Supporting Information and the model parameters can be found in Table 1.

Briefly, it has been assumed that the transport is diffusion dominated and that advective transport can be neglected, which is consistent with previous studies of organic contaminant transport at the site (Johnson et al., 1989; Myrand et al., 1992; Parker, 1996). Sorption was represented by the non-linear Freundlich isotherm as justified by our multistep sorption experiment (see section 4.1.) and by previous studies at the site for similar chlorinated hydrocarbon compounds (Allen-King et al., 1996, 1997; Johnson et al., 1989; Myrand et al., 1992). To compare simulated with measured concentration profiles, the simulated profiles were converted to total concentrations by using the following relationship (Parker et al., 2004):

$$C_{tot} = C_e \frac{R \cdot \Phi}{\rho_{wet}} \tag{4}$$

where, C_{tot} (mg/kg) corresponds to the total (sorbed and dissolved) concentration in the clay, C_e (mg/L) is the pore water concentration, ρ_{wet} (g/cm^3) refers to the sediment wet bulk density, ϕ (−) refers to the clay porosity, R (-) corresponds to the non-linear retardation factor (eq. (5), Supporting Information) as justified by the multistep sorption experiment (see section 4.1.) and ρ_{dry} (g/cm^3) refers to the dry bulk density. Parameter values, which were used to convert pore water to total concentrations were taken from a previous study at the site (Parker, 1996) (Table 1).

To simulate isotope ratio profiles of 1,2-DCA and DCM, isotopocules were considered as fractionation occurs between species of chlorinated hydrocarbon that differ in their isotopic composition and not between isolated isotopes. The term isotopocules encompasses isotopologues (molecules differing in isotopic composition) as well as isotopomers (molecules having the same number of isotopes but at different positions). Each 1,2-DCA and DCM carbon and 1,2-DCA chlorine isotopocules differing by one heavy isotope was defined as individual species in the model database (Tables 1 and 2 in Supporting Information). To account for isotopocule fractionation due to aqueous phase diffusion and sorption during the migration in the water-saturated clay, different Freundlich constants (K_{Fr}) and diffusion coefficients were assigned to each carbon and chlorine isotopocule differing in one heavy isotope (see section 2.1. in Supporting Information). The different Freundlich constants and diffusion coefficients were determined based on experimentally derived isotope fractionation factors for sorption and diffusion, which are proportional to the ratio of diffusion coefficients and Freundlich constants for isotopocules differing by one heavy isotope (Wanner and Hunkeler, 2015) (Table 3). To compare modelled isotopocule ratios with measured isotope ratio profiles, carbon and chlorine isotopocules differing by one heavy isotope were simulated in separate runs. Afterwards they were converted to isotope ratios by making use of the proportional behavior during the migration in low permeability sediments between isotopes and isotopocule pairs differing in one heavy isotope (Wanner and Hunkeler, 2015):

$$\delta^{37}Cl_{1,2-DCA}(z) = \left(\frac{\frac{I_{100}(z)+2I_{102}(z)}{2I_{98}(z)+I_{100}(z)}}{R_{SMOC}} - 1 \right) \cdot 1000 \tag{5}$$

$$\delta^{13}C_{1,2-DCA}(z) = \left(\frac{\frac{I_{100}(z)+2I_{101}(z)}{2I_{99}(z)+I_{100}(z)}}{R_{VPDB}} - 1 \right) \cdot 1000 \tag{6}$$

Table 1
Model Parameters for simulating the migration of chlorinated hydrocarbons in the Lambton Clay Plain at the permitted hazardous waste disposal site located close to Sarnia in Ontario, Canada.

Parameter	Unit	Value	Reference
Porosity:	–	0.34	(Parker, 1996)
Soil dry bulk density: ρ_{bdry}	g/cm^3	1.71	(Parker, 1996)
Soil wet bulk density: ρ_{bwet}	g/cm^3	2.02	(Parker, 1996)
Tortuosity[b]	–	0.91	Present study
Diffusion coefficient in free solution 1,2-DCA: $D_{0,1,2\text{-}DCA}$	m^2/s	9.90E-10	(USEPA, 1989)
Diffusion coefficient in free solution DCM: $D_{0,DCM}$	m^2/s	1.17E-09	(USEPA, 1989)
Freundlich sorption constant $K_{Fr,1,2\text{-}DCA}$[a]	$mg^{1-1/n}\ kg^{-1}\ L^{1/n}$	5.36	Present study
Freundlich sorption constant $K_{FR,DCM}$[a]	$mg^{1-1/n}\ kg^{-1}\ L^{1/n}$	2.97	Present study
Freundlich exponent 1/N 1,2-DCA[a]	–	0.74	Present study
Freundlich exponent 1/N DCM[a]	–	0.71	Present study
Initial 1,2-DCA boundary concentration (DNAPL saturated)	mg/L	8690	(Wiedemeier, 1999)
Initial DCM boundary concentration (DNAPL saturated)	mg/L	15,400	(Wiedemeier, 1999)
Start of boundary concentration decrease 1,2-DCA[b]	years	9.5	Present study
Start of boundary concentration decrease DCM[b]	years	10	Present study
Boundary concentration to which 1,2-DCA decreased[b]	mg/L	86.5	Present study
Boundary concentration to which DCM decreased[b]	mg/L	7700	Present study

[a] Experimentally determined.
[b] Calibrated.

$$\delta^{13}Cl_{DCM}(z) = \left(\frac{\frac{I_{88}(z)}{I_{87}(z)}}{R_{VPDB}} - 1\right)\cdot 1000 \quad (7)$$

where $\delta^{13}C$ and $\delta^{37}Cl$ are the carbon and chlorine delta values as a function of depth, I_x refers to the isotopocule abundance as a function of depth and R_{VPDB} and R_{SMOC} correspond to the international reference standard for carbon ($^{13}C/^{12}C = 0.011237$) and chlorine ($^{37}Cl/^{35}Cl = 0.32$) isotope ratios, respectively (Aelion et al., 2010).

The 2D numerical model domain (5 m length and 1 m width) was larger than the zone in which chlorinated hydrocarbons where detected to avoid boundary effects (Fig. 1, Supporting Information). The initial concentration at the location, where the DNAPL was present corresponded to the literature reported solubility limits for 1,2-DCA (8690 mg/L (Wiedemeier, 1999)) and DCM (15,400 mg/L (Wiedemeier, 1999)), respectively, while at the other end and on the vertical side of the modeling domain the concentration was set to zero. The abundance of carbon and chlorine isotopocules used in the boundary conditions was specified based on the measured isotope ratios adjacent to the source zone using a binominal distribution combining the occurrence of both C and Cl isotopes as proposed by Jin et al. (2013) (Tables 1 and 2, Supporting Information). Model calibration was conducted against measured concentration profiles, while the isotope ratio profiles were predicted based on the laboratory derived isotope fractionation factors for diffusion and sorption without further calibration. Manual calibration of concentration profiles was conducted by varying the D_e/D_0 ratio (eq. (4), Supporting Information), by setting the point in time when the boundary concentrations started to decrease (due to DNAPL exhaustion) and by the extent of the boundary concentration decrease following a smoothed step function at the location, where the DNAPL was present (Table 1). To quantify the quality of the fit between measured and modeled data, the Nash Sutcliff efficiency (NSE) was used. NSE values range between -∞ and 1, while 1 indicates a perfect fit between measured and modelled data.

4. Results

4.1. Multistep sorption experiment

During the performance of the multistep sorption experiment the aqueous phase concentration dropped by about six orders of magnitude due to sorption to the clay during each step (Fig. 2A and B). For both compounds 1,2-DCA and DCM, non-linear sorption occurred following the Freundlich isotherm (Freundlich, 1909) (Fig. 2A and B):

$$\log q_e = \log K_{Fr} + \frac{1}{N}\log C_e \quad (8)$$

where q_e (mg/kg-dry) and C_e (mg/L) are the equilibrium sorbed and solution concentrations, respectively, K_{Fr} ($mg^{1-1/n}\ kg^{-1}\ L^{1/n}$) refers to the Freundlich sorption coefficient and 1/N (-) is an empirical exponent indicating the degree of non-linearity.

Freundlich isotherm parameters of $K_{FR} = 5.36 \pm 0.35\ mg^{1-1/n}\ kg^{-1}\ L^{1/n}$ and $1/N = 0.74 \pm 0.05$ for 1,2-DCA and of $K_{FR} = 2.97 \pm 0.33\ mg^{1-1/n}\ kg^{-1}\ L^{1/n}$ and $1/N = 0.71 \pm 0.08$ for DCM were obtained (eq. (8); Table 2).

To compare the amount of sorption for 1,2-DCA and DCM, the unified Freundlich sorption variable was determined (Chen et al., 1999) as Freundlich constants with different degrees of non-linearity (1/N values) cannot be compared:

$$K_u = \frac{K_{Fr}}{C_e^{(N-1)/N}} \quad (9)$$

where K_u (L/kg) is the unified sorption variable for Freundlich isotherms.

The calculated K_u values (eq. (9)) for concentrations between 0 and 5000 mg/L indicate that 1,2-DCA sorbs stronger than DCM on the clay at the permitted hazardous waste disposal site (Fig. 2C), which is consistent with the higher value of the carbon-pore water partitioning coefficient (K_{OC}) for 1,2-DCA compared to DCM (Mabey et al., 1982).

During the multistep sorption experiment 1,2-DCA and DCM became increasingly enriched in heavy carbon (^{13}C) and chlorine isotopes (^{37}Cl) after each sorption step (Fig. 3A–C) showing that 1,2-DCA and DCM isotopocules with light isotopes are preferentially sorbed compared to isotopocules with heavy isotopes. To quantify the isotope fractionation factor for sorption following the Freundlich isotherm, the term $^{H}K_d/^{L}K_d$ in equation (1) was replaced by the ratio of the unified Freundlich sorption variable $^{H}K_u/^{L}K_u$ for the heavy and the light isotope, respectively:

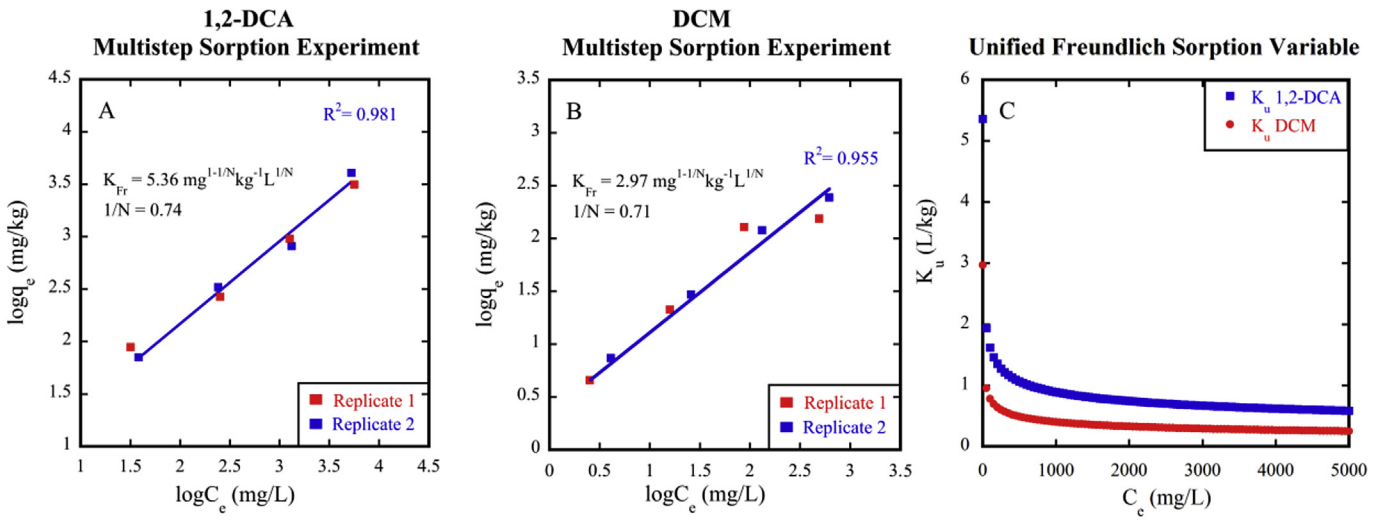

Fig. 2. Concentration in solution C_e (mg/L) vs. the sorbed concentration on the clay q_e (mg/kg-dry) for 1,2-DCA (A) and for DCM (B). Freundlich isotherm parameter (K_{Fr} and 1/N) for 1,2-DCA and DCM were determined using linear regression. Comparison of the sorption behaviour of 1,2-DCA and DCM using the unified Freundlich variable K_u (eq. (9)) as a function of the concentration in solution (C_e) (C).

Table 2
Determined parameters for the Freundlich isotherm for the low permeability sediments of the Lambton Clay Plain at the permitted hazardous waste disposal site located close to Sarnia in Ontario, Canada. Uncertainty of Freundlich constant (K_{Fr}) and exponent (1/N) was determined based on the 95% confidence interval of the regression line (eq. (8)).

Compound	K_{Fr} ($mg^{1-1/N}$ kg^{-1} $L^{1/n}$)	1/N (-)
1,2-DCA	5.36 ± 0.35	0.74 ± 0.05
DCM	2.97 ± 0.33	0.71 ± 0.08

$$\alpha_{sorption} = \frac{{}^{H}K_u}{{}^{L}K_u} = \frac{\frac{{}^{H}K_{Fr}}{C_e^{(N-1)/N}}}{\frac{{}^{L}K_{Fr}}{C_e^{(N-1)/N}}} = \frac{{}^{H}K_{Fr}}{{}^{L}K_{Fr}} \approx 1 + \Delta\delta_i/[1000m(1 - X_{dissolved})] \quad (10)$$

where ${}^{H}K_{Fr}$ and ${}^{L}K_{Fr}$ ($mg^{1-1/N}$ kg^{-1} $L^{1/N}$) are the Freundlich constants for the heavy and light isotope, respectively. Equation (10) shows that the isotope fractionation factor for sorption according to the Freundlich isotherm reduces to the ratio of the Freundlich constants ${}^{H}K_{Fr}/{}^{L}K_{Fr}$ of the heavy and light isotope, respectively.

For 1,2-DCA a larger enrichment of heavy chlorine compared to carbon isotopes was observed resulting in isotope fractionation factors of $\alpha_{Cl,sorption}$ = 0.99945 ± 0.00013 (eq. (10)) ($\varepsilon_{Cl,sorption}$ = −0.55‰; whereby $\varepsilon = (\alpha - 1)\cdot 1000$) and $\alpha_{C,sorption}$ = 0.99960 ± 0.00006 ($\varepsilon_{C,sorption}$ = −0.40‰), respectively (Table 3). For DCM the enrichment of heavy carbon isotope was larger compared to 1,2-DCA with $\alpha_{C,sorption}$ = 0.99946 ± 0.00017 ($\varepsilon_{C,sorption}$ = −0.54‰) (Table 3).

4.2. Diffusion cell experiment

During the diffusion cell experiment the initial and final concentration after each time series was used to determine the effective diffusion coefficient (D_e) according to Wanner and Hunkeler (2015). The ratio between initial and final DCM aqueous concentration ranged between 0.19 and 0.86 for the different time series of the diffusion cell experiments (Table 4). The average effective diffusion coefficient for DCM of the different time series was 1.06E-10 ± 1.78E-12 (m^2/s) (Table 4), which is lower than the diffusion coefficients in free solution (1.17E-09 m^2/s (USEPA, 1989)) as the frit reduces the diffusive transport rate due to porosity and tortuosity effects (eq. (4), Supporting Information). An enrichment of heavy DCM carbon isotopes in the source reservoir was observed (Fig. 4).

This indicates that the DCM carbon isotopocules with light isotopes diffuses faster out of the source reservoir than isotopocules with heavy carbon isotopes. The magnitude of DCM carbon isotope fractionation due to diffusion was quantified from the slope of the regression line using the Rayleigh equation (eq. (2)), resulting in an isotope fractionation factor of $\alpha_{C,diffusion}$ = 0.99972 ± 0.00009 ($\varepsilon_{C,diffusion}$ = −0.28‰) (Table 3).

Table 3
Determined fractionation factors for sorption and diffusion for carbon isotopocules of 1,2-DCA and DCM and for chlorine isotopocule of 1,2-DCA differing by one heavy isotope. Uncertainty of the fractionation factors due to sorption was calculated with the Gaussian error propagation law by taking into account the uncertainty (standard error of the mean) of the isotope ratio and the remaining fraction measurements after each sorption step (eq. (10)). Uncertainty for diffusion coefficient ratios was calculated based on the 95% confidence interval of the regression line (eq. (2)).

Compound	Isotopocule type	Fractionation factor sorption ($\alpha_{Sorption} = K_{Fr,i}/K_{Fr,j}$)	Fractionation factor diffusion ($\alpha_{Diffusion} = D_i/D_j$)
1,2-DCA	Carbon	$\alpha_{Sorption} = K_{Fr,100}/K_{Fr,99} = K_{Fr,101}/K_{Fr,100}$ = 0.99960 ± 0.00006[b]	$\alpha_{Diffusion} = D_{100}/D_{99} = D_{101}/D_{100}$ = 0.99977 ± 0.00004[a]
	Chlorine	$\alpha_{Sorption} = K_{Fr,100}/K_{Fr,98} = K_{Fr,102}/K_{Fr,100}$ = 0.99945 ± 0.00013[b]	$\alpha_{Diffusion} = D_{100}/D_{98} = D_{102}/D_{100}$ = 0.99939 ± 0.00003[a]
DCM	Carbon	$\alpha_{Sorption} = K_{Fr,88}/K_{Fr,87}$ = 0.99946 ± 0.00017[b]	$\alpha_{Diffusion} = D_{88}/D_{87}$ = 0.99972 ± 0.00009[b]

[a] Determined by Wanner and Hunkeler (2015).
[b] Determined by the present study.

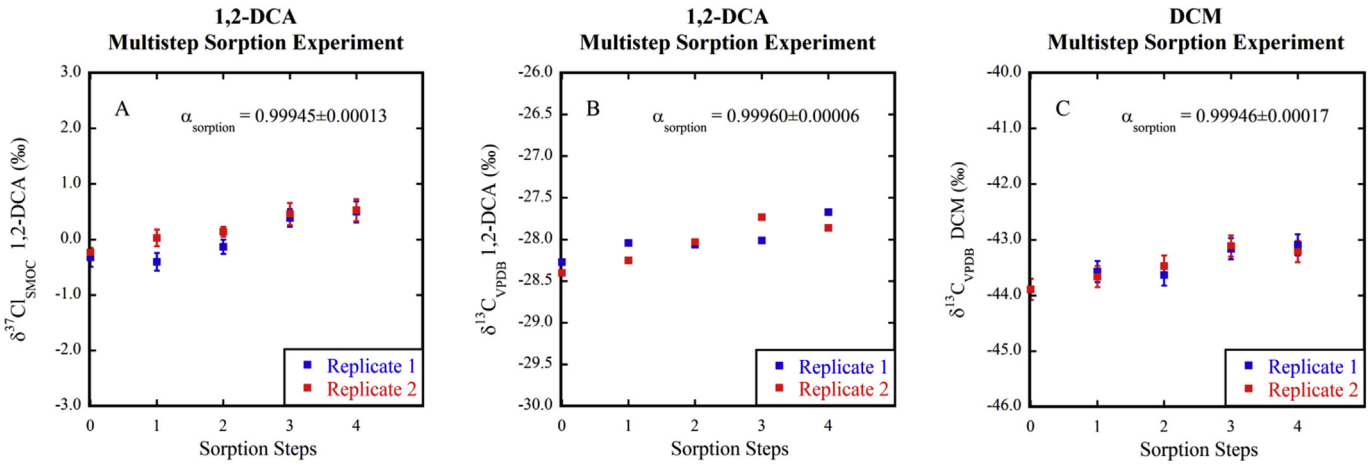

Fig. 3. Determination of the isotope fractionation factor due to sorption for chlorine (A) and carbon (B) isotopes of 1,2-DCA and for carbon isotopes of DCM (C). Error bars indicate analytical measurement uncertainty (standard error of the mean: SDM = 1σ/(n)1/2 σ: standard deviation n: sample number). For 1,2-DCA carbon isotopes (B) the analytical uncertainty was smaller than the size of the symbols in the plot. The uncertainty of the sorption-induced isotope fractionation factor was determined using the Gaussian error propagation law in equation (8) by including the uncertainty (±SDM) of the isotope ratio and the remaining fraction measurements after each sorption step.

Table 4
Effective diffusion coefficients and De/D_0 ratios of DCM for the diffusion cell experiment. Uncertainty of average diffusion coefficient was calculated by using the standard error of the mean (±SDM).

Initial (mg/L)	Final (mg/L)	Fraction	Time (d)	Effective diffusion coefficient (m^2/s)	Average effective diffusion coefficient (m^2/s)	D_e/D_0	D_e/D_0 average
15.5	8.8	0.566	10.1	1.10E-10		0.09	
58.8	50.7	0.862	3.3	8.86E-11		0.08	
324	98.4	0.303	22.3	1.04E-10		0.09	
416	80.4	0.193	25.9	1.23E-10	1.06E-10 ± 1.78E-12	0.11	0.09

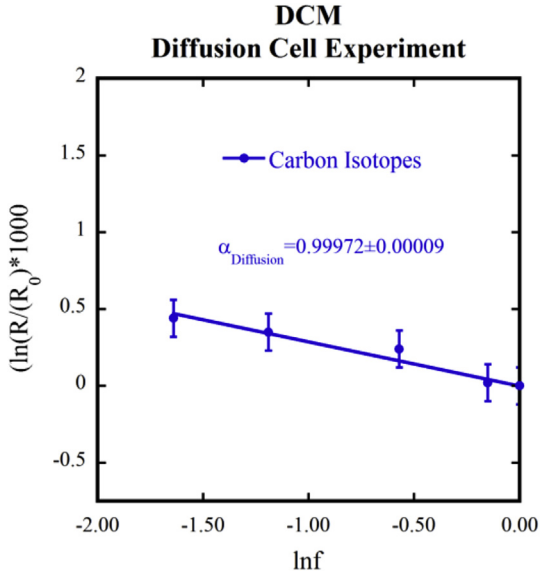

Fig. 4. Rayleigh plot for DCM carbon isotope fractionation in the source reservoir of the diffusion cell experiment. Error bars indicate analytical uncertainty (standard error of the mean: SDM = 1σ/(n)1/2 σ: standard deviation n: sample number) of measurements. Uncertainty of diffusion-induced isotope fractionation factor was calculated based on the 95% confidence interval of the regression line.

4.3. Concentration and compound-specific isotope profiles beneath the emplaced DNAPL sources

The determined 1,2-DCA and DCM concentration profiles in the clay unit below the emplaced DNAPL sources showed typical transient-diffusion profiles (Figs. 5A and 6A). The highest 1,2-DCA concentration (800 mg/kg) occurred at 18 cm vertical distance from the emplaced DNAPL source, while the concentration decreased below detection limit (<0.05 mg/kg) at 100 cm below the bottom of the emplaced source (Fig. 5A). The 1,2-DCA carbon and chlorine isotope ratio profiles showed trends in opposite directions, whereby ^{37}Cl in 1,2-DCA became depleted ($\Delta\delta^{37}Cl = 1.3‰$; Fig. 5B) and ^{13}C enriched ($\Delta\delta^{13}C = 1.9‰$; Fig. 5C) with increasing depth. The DCM concentration was highest adjacent to the DNAPL source and declined below the detection limit (<0.05 mg/kg) at 160 cm distance below the bottom of the emplaced source (Fig. 6A). DCM became enriched in ^{13}C with depth to the same extent ($\Delta\delta^{13}C = 2.4‰$) as 1,2-DCA ($\Delta\delta^{13}C = 1.9‰$) (Figs. 5C and 6B).

5. Discussion

5.1. Multistep sorption and diffusion cell experiment

The non-linear sorption behavior in the multistep sorption experiment is consistent with previous studies at the site, which also observed a Freundlich sorption trend with a similar degree of non-linearity (Allen-King et al., 1996, 1997). Furthermore, the multistep sorption experiment showed for the first time that isotope fractionation due to sorption occurs not only for carbon but also for chlorine isotopes for organic compounds.

The observed preferential sorption of isotopocules with light isotopes compared to isotopocules with heavy isotopes and the detected magnitude of isotope fractionation ($\alpha_{Sorption} = 0.99960–0.99945$; $\varepsilon_{Sorption} = -0.40‰$ to $-0.55‰$) for 1,2-DCA and DCM is coherent with previous experimental studies ($\alpha_{Sorption} = 0.99987–0.99896$; $\varepsilon_{Sorption} = -0.13‰$ to $-1.04‰$) conducted for carbon and hydrogen isotopes of benzene, toluene,

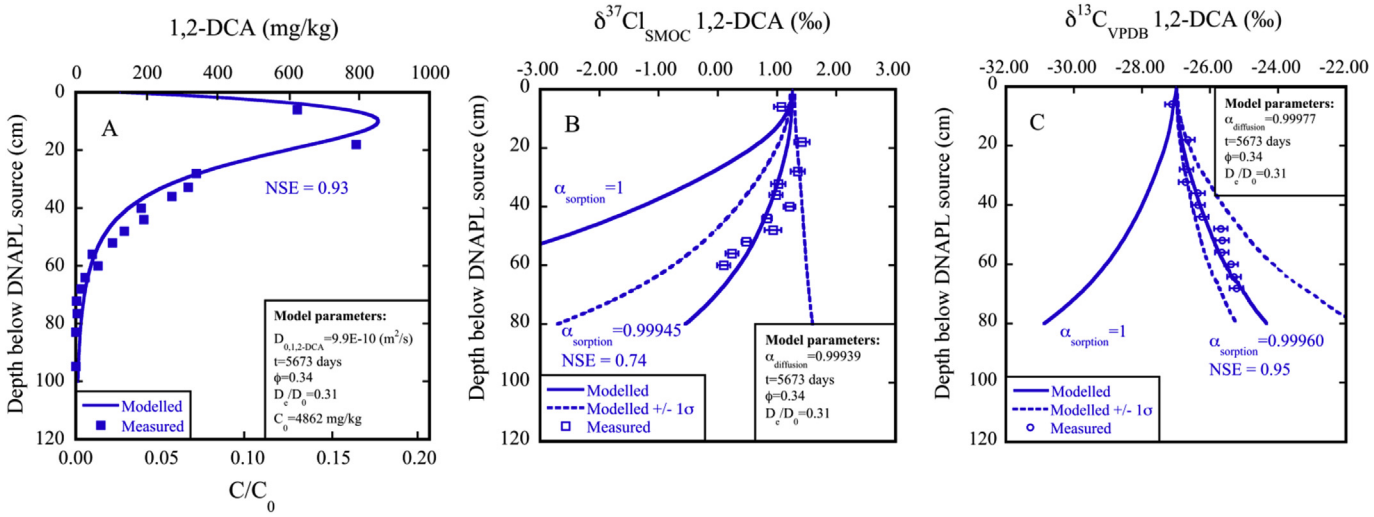

Fig. 5. 1,2-DCA total concentration profile (A), 1,2-DCA chlorine (B) and carbon (C) isotope ratio profiles below the DNAPL source in the retrieved clay core 5673 days after emplacement of the 1,2-DCA DNAPL source. The continuous lines represent the modelled concentration and isotope ratio profiles, while the filled squares (A), the open squares (B) and the open circles (C) represent the measured concentration and the isotope ratios in the depth-discrete samples. C_0 corresponds to the soil concentration at 1,2-DCA DNAPL pore water saturation (A). Dashed lines in figures B and C indicated sensitivity analysis of the uncertainty ($\pm 1\sigma$) of the sorption-induced isotope fractionation factors. For the 1,2-DCA chlorine and carbon isotopes two scenarios were simulated: Diffusion only ($\alpha_{sorption} = 1$) and a combined scenario that includes diffusion and sorption-induced isotope fractionation for 1,2-DCA chlorine ($\alpha_{sorption} = 0.99945$) and carbon ($\alpha_{sorption} = 0.99960$) isotopes (B and C). The Nash-Sutcliff efficiency (NSE) was used to quantify the quality of the fit between measured and modelled data.

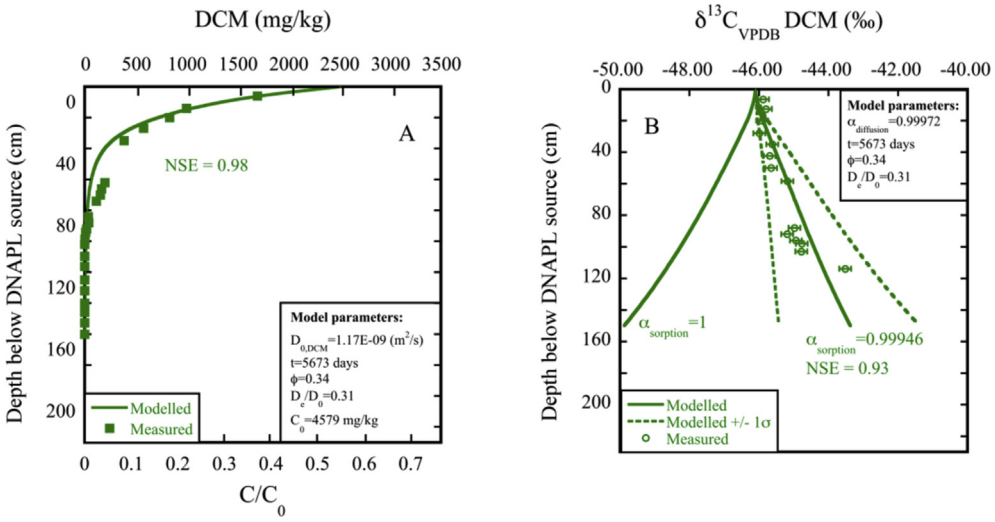

Fig. 6. DCM total concentration profile (A) and carbon isotope ratio profile (B) below the DNAPL source in the retrieved clay core 5673 days after emplacement of the DCM DNAPL source. The continuous lines indicate the modelled concentration and isotope ratios profiles, while the filled squares (A) and the open circles (B) represent the measured concentrations and the isotope ratios in the depth-discrete samples. C_0 corresponds to the soil concentration at DCM DNAPL pore water saturation (A). Dashed lines in figure B indicate sensitivity analysis of the uncertainty ($\pm 1\sigma$) of sorption-induced isotope fractionation factor. For the DCM carbon isotopes two scenarios were simulated: Diffusion only ($\alpha_{sorption} = 1$) and a combined scenario, which includes diffusion and sorption-induced isotope fractionation ($\alpha_{sorption} = 0.99946$) (B). The Nash-Sutcliff efficiency (NSE) was used to quantify the quality of the fit between measured and combined simulation scenario.

trichloroethene (Höhener and Yu, 2012; Imfeld et al., 2014; Kopinke et al., 2005). Furthermore, as after the first sorption step the shifts of isotope ratios remained within the analytical uncertainty of about 0.5‰, our multistep sorption experiment shows that a single step sorption experiment is not sufficient to detect sorption-induced isotope fractionation. This is in agreement with the studies conducted by Slater et al. (2000) and Schüth et al. (2003), which observed no significant sorption-induced isotope effect by performing a single step sorption experiment.

Isotope effects due to phase transition of hydrophobic compounds mainly occur due to changes of vibrational frequencies of the solute molecules caused by changing nonbonding interactions (Aelion et al., 2010; Jancso and Van Hook, 1974; Jeannottat and Hunkeler, 2012, 2013; Turowski et al., 2003). Accordingly, the detected preferential sorption of isotopocules with light compared to isotopocules with heavy isotopes can be likely explained by changes of vibrational frequencies due to changing nonbonding interactions during the transition between the aqueous solution and the sorbent material. In the sorbent material vibrational frequencies of the chlorinated hydrocarbon molecules are reduced compared to the aqueous solution due to the stronger interactions of the molecules with sorbent material (Turowski et al., 2003).

Consequently, the zero point energy levels of the light and heavy isotopocules are lower and closer together in the sorbent material than in the aqueous solution. As a result, the difference of zero point energies between sorbed and dissolved compounds in the aqueous solution is lower for heavy than for light isotopocules and thus, it takes slightly less energy for the heavy isotopocule to go into the aqueous phase than for the light isotopocules leading to a depletion of heavy isotopocules in the sorbent material. This isotope effect is similar as observed for air – water partitioning and DNAPL – vapor equilibration, during which also the reduction of vibrational frequencies in the water phase or in the DNAPL lead to a preferential transition of heavy carbon isotopocules to the gas phase compared to light isotopocules (Jeannottat and Hunkeler, 2012, 2013).

For the diffusion cell experiment, the observed faster diffusive transport rate for isotopocules with light compared to the heavy DCM carbon isotopes is in agreement with previous studies (Eggenkamp and Coleman, 2009; Richter et al., 2006; Wanner and Hunkeler, 2015). Furthermore, the determined magnitude of DCM carbon isotope fractionation due to diffusion is consistent with an earlier study (Wanner and Hunkeler, 2015), which investigated carbon and chlorine isotope fractionation of TCE and 1,2-DCA due to aqueous phase diffusion and obtained isotope fractionation factors in the same range ($\alpha_{Diffusion}$ = 0.99939–0.99978; $\varepsilon_{Diffusion}$ = −0.61‰ to −0.22‰) as the present study ($\alpha_{Diffusion}$ = 0.99972; $\varepsilon_{Diffusion}$ = −0.28‰). Moreover, the mass dependency of the diffusive transport rate (D) of the carbon isotopes of DCM showed a weaker power mass dependency ($D = m^{-0.025}$) than previously postulated by the kinetic theory ($D = m^{-0.5}$). This is in agreement with previous experiments (Eggenkamp and Coleman, 2009; Pikal, 1972; Richter et al., 2006; Rodushkin et al., 2004; Schloemer and Krooss, 2004; Tyroller et al., 2014; Wanner and Hunkeler, 2015; Zhang and Krooss, 2001) and molecular dynamic simulation studies (Bourg et al., 2010; Bourg and Sposito, 2007, 2008). Hence, the results of the diffusion cell experiment emphasized the failure of the kinetic theory for estimating the magnitude of isotope fractionation due to aqueous phase diffusion.

5.2. Concentration and compound-specific isotope diffusion profiles beneath the emplaced DNAPL sources

The greater vertical migration distance of DCM (160 cm) compared to 1,2-DCA (100 cm) is coherent with the results of the multistep sorption experiment, which revealed a stronger sorption behaviour of 1,2-DCA compared to DCM (Fig. 2C). Furthermore, the presence of the highest 1,2-DCA concentration below and not adjacent to the contamination source in the clay unit indicates that upward diffusion (i.e. back-diffusion) occurred due to the depletion of the contamination source, as it has been observed at other contaminated sites (Chapman and Parker, 2005). In contrast, the highest DCM concentration was detected adjacent to the emplaced source, suggesting the DCM DNAPL mass in the source zone had not decreased sufficiently to initiate back-diffusion. For DCM, the mass flux away from the source is expected to be smaller than for 1,2-DCA, because the concentration gradient is flatter due to weaker sorption. The enrichment of heavy carbon isotopes in 1,2-DCA and DCM with depth (Figs. 5C and 6B) is opposite to the isotope trend expected for the diffusive transport process (Wanner and Hunkeler, 2015). Isotope fractionation due to degradation can be excluded, as neither the present study nor a previous study (Parker, 1996) found evidence for reactive processes at the site. Furthermore, for reactive processes the decrease in concentration with depth would be associated with a greater isotope effect due to the large carbon isotope enrichment factors for 1,2-DCA (−3.5 to −32.0‰ (Palau et al., 2014)) and DCM (-41.2 to −66.3‰ (Nikolausz et al., 2006)) degradation, respectively. Thus, the observed isotope trend is likely caused by sorption. This conclusion is supported by the results of the multistep sorption experiment, which showed that the sorbed compounds are depleted in heavy isotopes, enhancing the mobility of isotopocules with heavy isotopes in the clay unit and leading to an enrichment of heavy isotopes with depth. However, in contrast to carbon isotopes, the 1,2-DCA chlorine isotopes show an opposite isotope trend towards lighter signatures with depth. The opposite isotope trend for Cl compared to C isotopes reinforces the hypothesis that degradation is absent as no inverse degradation-induced isotope effect for chlorine isotopes is known. As the mass difference is two between stable chlorine compared to one for carbon isotopes, the diffusive isotope effect is stronger for the chlorine compared to carbon isotopes. Therefore, the trend towards lighter signatures with depth for 1,2-DCA chlorine isotopes could be explained by the interaction between sorption and diffusion, whereby the diffusion isotope effect overrules the sorption effect. To evaluate the relative contribution of sorption and diffusion in more detail, numerical modeling was used as discussed in the following section.

5.3. Simulation of field site-derived concentration and compound-specific isotope profiles

The 2D axisymmetrical numerical model was applied a) to assess if measured 1,2-DCA and DCM concentration profiles can be reproduced with the experimentally determined parameters for the non-linear Freundlich isotherm (Table 2, Fig. 2A and B); and b) to investigate if and how isotope fractionation due to diffusion and sorption processes are superimposed in water-saturated low permeability sediments.

Simulated 1,2-DCA and DCM concentration profiles agreed well with measured concentration profiles (Figs. 5A and 6A). The best fit for the 1,2-DCA (NSE = 0.93) and for the DCM (NSE = 0.98) concentration profiles was obtained with a D_e/D_0 ratio of 0.31 (eq. (4), Supporting Information) and with a start of the concentration decrease at the source zone at 9.5 (1,2-DCA) and 10 years (DCM) after source emplacement to pore water concentrations of 86.5 mg/L for 1,2-DCA and of 7700 mg/L for DCM, respectively (Table 1). The consistency between measured and modelled 1,2-DCA and DCM concentration data confirms that non-linear sorption occurs, which is in agreement with the multistep sorption experiment and with previous studies at the site (Allen-King et al., 1996, 1997).

To assess the relative contribution of isotope fractionation due sorption and diffusion on isotope ratio profiles in the clay unit, two scenarios were simulated and compared with measured isotope ratio profiles: Isotope fractionation by a) diffusion only ($\alpha_{Sorption}$ = 1), and b) by a combination of diffusion and sorption. The diffusion only scenario was not in agreement with measured isotope ratio profiles. For the 1,2-DCA chlorine isotopes, the simulated shift with depth was larger than the measured (Fig. 5B), while for the 1,2-DCA and DCM carbon isotopes the simulated profiles showed an opposite trend compared to measured isotope profiles (Figs. 5C and 6B), suggesting that isotope fractionation occurs not only due to the diffusion. In contrast, for the simulation scenario including both sorption and diffusion-induced isotope fractionation, the simulated 1,2-DCA and DCM isotope profiles agreed well with the measured profiles (NSE = 0.74–0.95) (Fig. 5B–C and Fig. 6B). This further substantiates that sorption-induced isotope fractionation causes an enrichment of heavy 1,2-DCA and DCM carbon isotopes, and that for 1,2-DCA chlorine isotopes the stronger diffusion isotope effect overrides the sorption effect causing a trend towards lighter isotopes with depth. Furthermore, the direction of the shift of 1,2-DCA and DCM carbon isotope ratios (enrichment of

heavy isotopes) with depth does not change when varying the sorption-induced isotope fractionation factor within the uncertainty, which is related with isotope ratio and the remaining fraction measurements (±1σ; Figs. 5C and 6B). This underlines the conclusion that sorption causes the enrichment of heavy 1,2-DCA and DCM carbon isotopes with depth.

The amount of isotope fractionation due to sorption might not only depend on the magnitude of sorption isotope fractionation factor but also on the extent of sorption. To investigate how the extent of sorption influences isotope fractionation, the migration of 1,2-DCA in saturated low permeability sediments was simulated for different Freundlich constants (K_{Fr}) ranging between 2 and 10 (Fig. 7A and B). The simulations were conducted for a constant 1,2-DCA source concentration at 1,2-DCA DNAPL pore water saturation (C_0 = 8690 mg/L) and for the same time period as the field experiments (5673 days). By plotting simulated 1,2-DCA carbon and chlorine isotope profiles for different K_{Fr} values against 1,2-DCA concentrations normalized to the source concentration (C/C_0) on a logarithmic scale, it becomes apparent that a stronger sorption behavior leads to a steeper concentration gradient, which amplifies the isotope trend going in opposite directions (Fig. 7A and B). For the 1,2-DCA chlorine isotopes, for which diffusion is the predominant fractionation process, a steeper concentration gradient is associated with a larger depletion of heavy chlorine isotopes with depth (Fig. 7A). In contrast, for the 1,2-DCA carbon isotopes, for which sorption dominates isotope fractionation, an augmentation of the extent of sorption leads to a larger enrichment of heavy isotopes with depth (Fig. 7B).

Sorption-induced isotope fractionation can potentially disturb the identification of reactive processes by using stable isotope methods. Shifts of isotope ratios can reach 2‰ (Fig. 5B–C and 6B), which is considered as a lower limit to provide solid evidence for reactive processes (Hunkeler et al., 2005). The disturbance might be especially relevant for carbon isotopes as sorption shifts carbon isotope ratios towards the same direction as reactive processes (enrichment of heavy isotopes with depth). To investigate the extent of disturbance, a degradation scenario was simulated with a relatively slow degradation rate (half-life = 506 days) associated with isotope fractionation factors ranging between 0.999 and 0.995. Furthermore, the degradation scenario was simulated without and with taking into account sorption-induced isotope fractionation. The degradation scenario was compared with 1,2-DCA and DCM carbon isotope ratio profiles as the observed magnitude of isotope fractionation due to sorption for 1,2-DCA and DCM carbon isotopes is expected to be representative for other hydrophobic organic compounds. In the degradation scenario with the smallest isotope fractionation factor (0.999), a similar shift of carbon isotope ratios with depth was observed as in the scenario without degradation (Fig. 8A and B). This indicates that for carbon isotope ratio profiles showing shifts of about $\Delta\delta^{13}C$ = 2.0‰ with depth, their attribution to degradation processes cannot be made unequivocally, especially in high organic content (high sorption capacity) sediments. Furthermore, the simulated profiles in the degradation scenario revealed that if sorption-induced isotope fractionation is ignored (considered negligible), the simulated enrichment of heavy isotopes with depth is less strong (Fig. 8A and B). Hence, when fitting a reactive transport model to measured carbon isotope ratio profiles by ignoring sorption-induced isotope fractionation, the total enrichment of heavy isotope with depth will be assigned to reactive processes. This leads to an overestimation of reaction rates. Therefore, isotope effects due to sorption should be considered for the identification and quantification of reactive processes by using stable isotope methods especially for slow reactions with small isotope fractionation factors.

6. Conclusions

This study provides for the first time clear evidence that isotope fractionation due to sorption has a measurable effect on carbon and chlorine isotope patterns of chlorinated hydrocarbons under field conditions in saturated low permeability sediments. By including laboratory determined enrichment factors for sorption and diffusion in a numerical model, laboratory and field observations in saturated low permeable units were consistently related. The results of the numerical model demonstrated that sorption and diffusion are superimposed and compensate each other to some degree as these processes fractionate isotopes in opposite directions. Hence, depending on whether sorption or diffusion shows the larger isotope fractionation factor, isotope ratios are shifted in opposite directions in aquitards. Moreover, an increased sorption extent leads to an amplification of the isotope trends. Furthermore, this study shows that sorption-induced isotope fractionation can cause shifts of isotope ratios of around 2‰ in saturated low permeable units, which is considered as a threshold value for identifying reactive processes affecting organic compounds (Hunkeler et al., 2008). Numerical modelling showed that specific

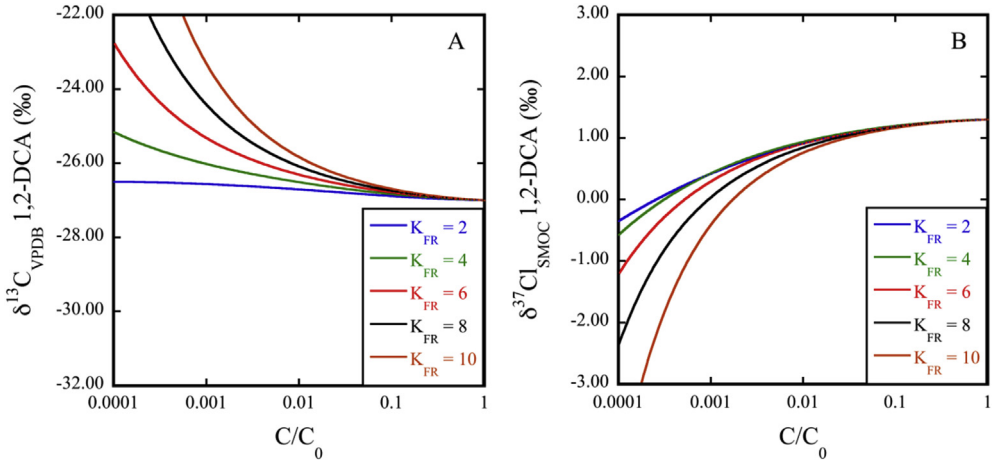

Fig. 7. Simulated 1,2-DCA chlorine (A) and carbon (B) isotope fractionation as function of the concentration normalized to the source concentration (C_0) on a logarithmic scale for different Freundlich constants (K_{Fr}) ranging between 2 and 10. The simulation was performed for a constant source concentration (C_0) at 1,2-DCA DNAPL pore water saturation (8690 mg/L) and for the same time period as for the field experiments (5673 days).

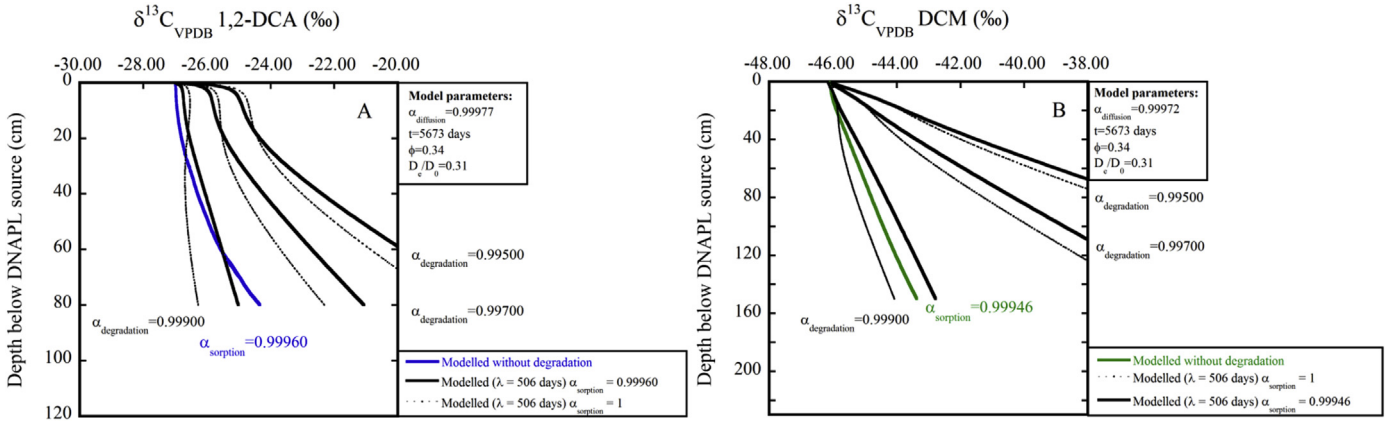

Fig. 8. Simulated 1,2-DCA (A) and DCM (B) carbon isotope ratio profiles by including reactive processes (black lines) with fraction factors ranging between 0.999 and 0.995 and a half-life (λ) of 506 days. The continuous black lines represent the reactive scenario in which sorption-induced isotope fractionation was included, while the black-dashed lines represent the reactive scenario in which sorption-induced isotope fractionation was neglected. The continuous blue (A) and green lines (B) correspond to the non-reactive scenario, which considers isotope fractionation due to sorption and diffusion only.

conditions (high sorption capacity, early transient diffusion state) can cause even larger shifts of isotope ratios due to sorption. Therefore, shifts of isotope ratios of around 2‰ in low permeable units are not unequivocally attributable to reactive processes. This is especially important for the identification of slow reactive processes associated with small degradation induced isotope fractionation factors Moreover, although this study was carried out in low-permeability sediments, it is expected that sorption-induced isotope fractionation has a similar magnitude in more permeable units, as sorption also occurs on organic matter. Hence, the data set of this study also provides a starting point to evaluate the relevance of sorption-induced isotope fractionation is such permeable units with the help of modelling approaches.

Acknowledgment

The authors acknowledge the Swiss National Science Foundation (SNFS) for financial support for this isotope focused study, as well as the University Consortium for Field-Focused Groundwater Contamination Research and the Natural Sciences and Engineering Research Council of Canada (NSERC) including a Discovery Grant to Dr. Parker for funding of the larger research effort. Furthermore, the authors thank Robert Ingleton and Paul Johnson from the University of Waterloo, who operated the Geoprobe rig and also supported the initial emplaced source installations. Several people from the University of Guelph, notably Ryan Kroeker, Dan Elliot and Keelin Scully also provided field support and Maria Gorecka and Rashmi Jadeja provided analytical support. The site operator Clean Harbors is also acknowledged for providing site access and field support for the research. Furthermore, the authors thank two anonymous reviewers for their valuable comments, which greatly helped to improve the quality of the manuscript.

Appendix A. Supplementary data

Supplementary data related to this article can be found at http://dx.doi.org/10.1016/j.apgeochem.2017.07.016.

References

Aelion, C.M., Höhener, P., Hunkeler, D., Aravena, R., 2010. Environmental Isotopes in Biodegradation and Bioremediation. CRC Press, USA, p. 450.
Allen-King, R.M., Groenevelt, H., Mackay, D.M., 1995. Analytical method for the sorption of hydrophobic organic pollutants in clay-rich materials. Environ. Sci. Technol. 29 (1), 148–153.
Allen-King, R.M., Groenevelt, H., Warren, C.J., Mackay, D.M., 1996. Non-linear chlorinated-solvent sorption in four aquitards. J. Contam. Hydrology 22 (3), 203–221.
Allen-King, R.M., McKay, L.D., Trudell, M.R., 1997. Organic carbon dominated trichloroethene sorption in a clay-rich glacial deposit. Groundwater 35 (1), 124–130.
Bourg, I.C., Richter, F.M., Christensen, J.N., Sposito, G., 2010. Isotopic mass dependence of metal cation diffusion coefficient in liquid water. Geochimica Cosmochimica 74, 2249–2256.
Bourg, I.C., Sposito, G., 2007. Molecular dynamics simulations of kinetic isotope fractionation during the diffusion of ionic species in liquid water. Geochimica Cosmochimica Acta 71 (23), 5583–5589.
Bourg, I.C., Sposito, G., 2008. Isotopic fractionation of noble gases by diffusion in liquid water: molecular dynamics simulations and hydrologic applications. Geochimica Cosmochimica Acta 72 (9), 2237–2247.
Caimi, R.J., Brenna, J.T., 1993. High-precision liquid chromatography-combustion isotope ratio mass spectrometry. Anal. Chem. 65 (23), 3497–3500.
Caimi, R.J., Brenna, J.T., 1997. Quantitative evaluation of carbon isotopic fractionation during reversed-phase high-performance liquid chromatography. J. Chromatogr. A 757 (1), 307–310.
Chapman, S.W., Parker, B.L., 2005. Plume persistence due to aquitard back diffusion following dense nonaqueous phase liquid source removal or isolation. Water Resour. Res. 41 (12).
Chen, Z., Xing, B., McGill, W., 1999. A unified sorption variable for environmental applications of the Freundlich equation. J. Environ. Qual. 28 (5), 1422–1428.
Desaulniers, D.E., Kaufmann, R.S., Cherry, J.A., Bentley, H.W., 1985. ^{37}Cl - ^{35}Cl variations in a diffusion-controlled groundwater system. Geochimica Cosmochimica 50, 1757–1764.
Eggenkamp, H.G.M., Coleman, M.L., 2009. The effect of aqueous diffusion on the fractionation of chlorine and bromine stable isotopes. Geochimica Cosmochimica Acta 73 (12), 3539–3548.
Einarson, M.D., Casey, M.B., Winglewich, D.L., Morkin, M.I., 1998. Enviro-core - a dual-tube direct push system for rapid site characterization. In: Proceedings of the Symposium on the Application of Geophysics to Environmental and Engineering Problems. Environmental & Engineering Geophysical Society, Wheat Ridge, pp. 1–10.
Elsner, M., Hunkeler, D., 2008. Evaluating chlorine isotope effects from isotope ratios and mass spectra of polychlorinated molecules. Anal. Chem. 80 (12), 4731–4740.
Elsner, M., Zwank, L., Hunkeler, D., Schwarzenbach, R.P., 2005. A new concept linking observable stable isotope fractionation to transformation pathways of organic pollutants. Environ. Sci. Technol. 39 (18), 6896–6916.
Filer, C.N., 1999. Isotopic fractionation of organic compounds in chromatography. J. Label. Compd. Radiopharm. 42 (2), 169–197.
Freundlich, H., 1909. The theory of adsorption. Z. Chem. Ind. Kolloide 3, 212–220.
Grathwohl, P., 1990. Influence of organic-matter from soils and sediments from various origins on the sorption of some chlorinated aliphatic-hydrocarbons - implications on K_{OC} correlations. Environ. Sci. Technol. 24 (11), 1687–1693.
Harrington, R.R., Poulson, S.R., Drever, J.I., Colberg, P.J.S., Kelly, E.F., 1999. Carbon isotope systematics of monoaromatic hydrocarbons: vaporization and adsorption experiments. Org. Geochem. 30 (8A), 765–775.
Holt, B.D., Sturchio, N.C., Abrajano, T.A., Heraty, L.J., 1997. Conversion of chlorinated volatile organic compounds to carbon dioxide and methyl chloride for isotopic analysis of carbon and chlorine. Anal. Chem. 69 (14), 2727–2733.
Huang, L., Sturchio, N.C., Abrajano, T., Heraty, L.J., Holt, B.D., 1999. Carbon and chlorine isotope fractionation of chlorinated aliphatic hydrocarbons by evaporation. Org. Geochem. 30 (8A), 777–785.

Hunkeler, D., Abe, Y., Broholm, M.M., Jeannottat, S., Westergaard, C., Jacobsen, C.S., Aravena, R., Bjerg, P.L., 2011. Assessing chlorinated ethene degradation in a large scale contaminant plume by dual carbon-chlorine isotope analysis and quantitative PCR. J. Contam. Hydrol. 119 (1–4), 69–79.
Hunkeler, D., Aravena, R., Berry-Spark, K., Cox, E., 2005. Assessment of degradation pathways in an aquifer with mixed chlorinated hydrocarbon contamination using stable isotope analysis. Environ. Sci. Technol. 39 (16), 5975–5981.
Hunkeler, D., Aravena, R., Butler, B.J., 1999. Monitoring microbial dechlorination of tetrachloroethene (PCE) in groundwater using compound-specific stable carbon isotope ratios: microcosm and field studies. Environ. Sci. Technol. 33 (16), 2733–2738.
Hunkeler, D., Meckenstock, R.U., Sheerwood Lollar, B., Schmidt, T.C., Wilson, J.T., 2008. A guide for assessing biodegradation and source identification of organic ground water contaminants using compound specific isotope analysis. Environental Prot. Agency (EPA) 600 (R-08), 68.
Hwang, Y.K., Endres, A.L., Piggott, S.D., Parker, B.L., 2008. Long-term ground penetrating radar monitoring of a small volume DNAPL release in a natural groundwater flow field. J. Contam. hydrology 97 (1), 1–12.
Höhener, P., Atteia, O., 2010. Multidimensional analytical models for isotope ratios in groundwater pollutant plumes of organic contaminants undergoing different biodegradation kinetics. Adv. Water Resour. 33 (7), 740–751.
Höhener, P., Yu, X., 2012. Stable carbon and hydrogen isotope fractionation of dissolved organic groundwater pollutants by equilibrium sorption. J. Contam. Hydrology 129, 54–61.
Imfeld, G., Kopinke, F.D., Fischer, A., Richnow, H.H., 2014. Carbon and hydrogen isotope fractionation of benzene and toluene during hydrophobic sorption in multistep batch experiments. Chemosphere 107, 454–461.
Jancso, G., Van Hook, W.A., 1974. Condensed phase isotope effects. Chem. Rev. 74 (6), 689–750.
Jeannottat, S., Hunkeler, D., 2012. Chlorine and carbon isotopes fractionation during volatilization and diffusive transport of trichloroethene in the unsaturated zone. Environ. Sci. Technol. 46 (6), 3169–3176.
Jeannottat, S., Hunkeler, D., 2013. Can soil gas VOCs be related to groundwater plumes based on their isotope signature? Environ. Sci. Technol. 47 (21), 12115–12122.
Jin, B., Haderlein, S.B., Rolle, M., 2013. Integrated carbon and chlorine isotope modeling: applications to chlorinated aliphatic hydrocarbons dechlorination. Environ. Sci. Technol. 47 (3), 1443–1451.
Johnson, R.L., Cherry, J.A., Pankow, J.F., 1989. Diffusive contaminant transport in natural clay: a field example and implications for clay-lined waste disposal sites. Environ. Sci. Technol. 23 (3), 340–349.
Klein, P., Simborg, D., Szczepanik, P.A., 1964. Detection and computation of isotope fractionation in the adsorption chromatography of dual-labelled compounds. Pure Appl. Chem. 8 (3–4), 357–370.
Kopinke, F.D., Georgi, A., Voskamp, M., Richnow, H.H., 2005. Carbon isotope fractionation of organic contaminants due to retardation on humic substances: implications for natural attenuation studies in aquifers. Environ. Sci. Technol. 39 (16), 6052–6062.
Kueper, B.H., Redman, D., Starr, R.C., Reitsma, S., Mah, M., 1993. A field experiment to study the behavior of Tetrachloroethylene below the water-table - spatial - distribution of residual and pooled DNAPL. Ground Water 31 (5), 756–766.
Liu, H., Li, Y.X., He, X., Sissou, Z., Tong, L., Yarnes, C., Huang, X.Y., 2016. Compound-specific carbon isotopic fractionation during transport of phthalate esters in sandy aquifer. Chemosphere 144, 1831–1836.
Lollar, B.S., Slater, G.F., Ahad, J., Sleep, B., Spivack, J., Brennan, M., MacKenzie, P., 1999. Contrasting carbon isotope fractionation during biodegradation of trichloroethylene and toluene: implications for intrinsic bioremediation. Org. Geochem. 30 (8), 813–820.
Mabey, W.R., Smith, J.H., Podoll, R.T., 1982. Aquatic Fate Process Data for Organic Priority Pollutants, vol. 440. US Environmental Protection Agency, Office of Water Regulations and Standards, Washington, DC EPA.
McKay, L., Fredericia, J., 1995. Distribution, origin, and hydraulic influence of fractures in a clay-rich glacial deposit. Can. Geotechnical J. 32 (6), 957–975.
Meckenstock, R.U., Morasch, B., Griebler, C., Richnow, H.H., 2004. Stable isotope fractionation analysis as a tool to monitor biodegradation in contaminated acquifers. J. Contam. Hydrology 75 (3–4), 215–255.
Myrand, D., Gillham, R., Sudicky, E., O'Hannesin, S., Johnson, R., 1992. Diffusion of volatile organic compounds in natural clay deposits: laboratory tests. J. Contam. Hydrology 10 (2), 159–177.
Nikolausz, M., Nijenhuis, I., Ziller, K., Richnow, H.H., Kästner, M., 2006. Stable carbon isotope fractionation during degradation of dichloromethane by methylotrophic bacteria. Environ. Microbiol. 8 (1), 156–164.
Palau, J., Cretnik, S., Shouakar-Stash, O., Hoche, M., Elsner, M., Hunkeler, D., 2014. C and Cl isotope fractionation of 1,2-dichloroethane displays unique $\delta^{13}C/\delta^{37}Cl$ patterns for pathway identification and reveals surprising C-Cl bond involvement in microbial oxidation. Environ. Sci. Technol. 48 (16), 9430–9437.
Pankow, J.F., Cherry, J.A., 1996. Dense Chlorinated Solvents and Other DNAPLs in Groundwater Waterloo. Press, Portland, OR., p. 522
Parker, B.L., 1996. Effect of Molecular Diffusion on the Persistence of Dense Immiscible Phase Organic Liquids in Fractured Porous Geologic Media. PhD Thesis. University of Waterloo, Waterloo, Ontario, Canada, 191 pp.
Parker, B.L., Chapman, S.W., Guilbeault, M.A., 2008. Plume persistence caused by back diffusion from thin clay layers in a sand aquifer following TCE source-zone hydraulic isolation. J. Contam. Hydrology 102 (1–2), 86–104.
Parker, B.L., Cherry, J.A., Chapman, S.W., 2004. Field study of TCE diffusion profiles below DNAPL to assess aquitard integrity. J. Contam. Hydrology 74 (1–4), 197–230.
Parker, B.L., Gillham, R.W., Cherry, J.A., 1994. Diffusive disappearance of immiscible-phase organic liquids in fractured geologic media. Groundwater 32 (5), 805–820.
Pikal, M.J., 1972. Isotope effects in tracer diffusion. comparison of the diffusion coefficients of $^{24}Na^{+}$ and $^{22}Na^{+}$ in aqueous electrolytes. J. Phys. Chem. 76, 3038–3040.
Poulson, S.R., Drever, J.I., Colberg, P.J., 1997. Estimation of K oc values for deuterated benzene, toluene, and ethylbenzene, and application to ground water contamination studies. Chemosphere 35 (10), 2215–2224.
Richter, F.M., Mendybaev, R.A., Christensen, J.N., Hutcheon, I.D., Williams, R.W., Sturchio, N.C., Beloso, A.D., 2006. Kinetic isotopic fractionation during diffusion of ionic species in water. Geochim. Cosmochim Acta 70 (2), 277–289.
Rivett, M.O., Allen-King, R.M., 2003. A controlled field experiment on groundwater contamination by a multicomponent DNAPL: dissolved-plume retardation. J. Contam. Hydrology 66 (1), 117–146.
Rodushkin, I., Stenberg, A., Andrén, H., Malinovsky, D., Baxter, D.C., 2004. Isotopic fractionation during diffusion of transition metal ions in solution. Anal. Chem. 76, 2148–2151.
Schloemer, S., Krooss, B.M., 2004. Molecular transport of methane, ethane and nitrogen and the influence of diffusion on the chemical and isotopic composition of natural gas accumulations. Geofluids 4 (1), 81–108.
Schwille, F., 1988. Dense Chlorinated Solvents in Porous and Fractured Media: Model Experiments. Boca Raton, FL, USA.
Schüth, C., Taubald, H., Bolaño, N., Maciejczyk, K., 2003. Carbon and hydrogen isotope effects during sorption of organic contaminants on carbonaceous materials. J. Contam. Hydrology 64 (3), 269–281.
Slater, G.F., Ahad, J.M.E., Lollar, B.S., Allen-King, R., Sleep, B., 2000. Carbon isotope effects resulting from equilibrium sorption of dissolved VOCs. Anal. Chem. 72 (22), 5669–5672.
Turowski, M., Yamakawa, N., Meller, J., Kimata, K., Ikegami, T., Hosoya, K., Tanaka, N., Thornton, E.R., 2003. Deuterium isotope effects on hydrophobic interactions: the importance of dispersion interactions in the hydrophobic phase. J. Am. Chem. Soc. 125 (45), 13836–13849.
Tyroller, L., Brennwald, M.S., Mächler, L., Livingstone, D.M., Kipfer, R., 2014. Fractionation of Ne and Ar isotopes by molecular diffusion in water. Geochimica Cosmochimica Acta 136, 60–66.
USEPA, 1989. Hazardous Waste Treatment, Storage, and Disposal Facilities (TSDF)-USEPA, OAQPS, Air Emission Models (EPA-450/3-87-026).
Van Breukelen, B.M., Prommer, H., 2008. Beyond the Rayleigh equation: reactive transport modeling of isotope fractionation effects to improve quantification of biodegradation. Environ. Sci. Technol. 42 (7), 2457–2463.
Voskamp, M., 2004. Untersuchungen zur Sorption an Huminstoffen: Molekulargewicht und Kohlenstoff-Isotopenfraktionierung. UFZ.
Wanner, P., Hunkeler, D., 2015. Carbon and chlorine isotopologue fractionation of chlorinated hydrocarbons during diffusion in water and low permeability sediments. Geochimica Cosmochimica Acta 157, 198–212.
Wanner, P., Parker, B.L., Chapman, S.W., Aravena, R., Hunkeler, D., 2016. Quantification of degradation of chlorinated hydrocarbons in saturated low permeability sediments using Compound-Specific Isotope Analysis. Environ. Sci. Technol. 50 (11), 5622–5630.
White, R.A., Rivett, M.O., Tellam, J.H., 2008. Paleo-roothole facilitated transport of aromatic hydrocarbons through a Holocene clay bed. Environ. Sci. Technol. 42 (19), 7118–7124.
Wiedemeier, T.H., 1999. Natural Attenuation of Fuels and Chlorinated Solvents in the Subsurface. John Wiley & Sons.
Zhang, T.W., Krooss, B.M., 2001. Experimental investigation on the carbon isotope fractionation of methane during gas migration by diffusion through sedimentary rocks at elevated temperature and pressure. Geochimica Cosmochimica Acta 65 (16), 2723–2742.